International Journal of Modern Manufacturing Technologies
ISSN 2067–3604, Vol. XI, No. 1 / 2019

ON ONE METHODOLOGY FOR CONTROLLING THE ACCURACY AND QUALITY OF THE SURFACE OF GEARS

Ivan Gostev[1, 2]

[1]Higher School of Economics" National Research University, Business Informatics School, Myasnitskaya Str., 20, Moscow, 101000, Russia
[2]A.A. Kharkevich Institute for Information Transmission Problems, Russian Academy of Sciences, The center of the distributed calculations, Bolshoy Karetny per. 19, build.1, Moscow, 127051 Russia

Corresponding author: Ivan Gostev, igostev@gmail.com

Abstract: Accuracy control in component processing is most important and relevant in mechanical engineering. Deviations from the specified shape leads to various malfunctions of the entire mechanical part of the system. So, for example, deviations of the tooth shape in gear leads to an increase in friction, which leads to an increase in heat generation, a decrease in the efficiency of the system, increased wear of a pair of gears, and ultimately to system failure. To control the shape of the teeth, an identification method based on the metric of a modified geometric correlation is proposed. This method involves scanning the object, pre-processing the resulting image, highlighting the necessary features, which are used to control the shape of the object. This technology allows determination of deviations from the shape of controlled objects with the required accuracy invariant to the shift, scaling, and rotation of the part. An advantage in this technology is that it is not necessary to position the camera precisely with respect to the scanned identified object.

Key words: Gear accuracy, measurement, metric, delta segmentation, shape quality, image processing, pattern recognition.

1. INTRODUCTION

If the object of measurement is directly accessible or if the velocity of the object motion allows for manual measurements, then there is a variety of such devices and techniques [1-3]. The task is much more difficult when it is impossible to make contact with the object. The existing systems for controlling the quality of the gear teeth shape allow controlling their shape, but using, e.g., involute profile measuring machines to control the actual profile of the face section of a tooth with a theoretical evolvent is often physically impossible or inefficient [4].
In addition, in simple control systems the process requires certain positioning of the part, and in more complex systems, remote control of the accuracy of the shape is in most cases based on expensive interferometers [5]. In the continuous production of parts, remote control of their shape should not depend on the position and orientation of the part on the conveyor relative to movement. To automate this process, one can use video monitoring, in which the object is scanned with the necessary resolution for a given accuracy. Then, after the image pre-processing, the surface geometry of the part is compared with the reference surface. However, it is necessary to ensure that the measurement accuracy is independent of the camera position, i.e., the measurements should be invariant to changes of the object image (magnification/reduction of the image, shift of the object within the frame, rotation relative to movement).
In the proposed technology, in order to ensure the required accuracy of the shape of parts, for example, the shape of the gear tooth, have been used following methods.
In this paper, we consider methodology for more quality detecting contour based on a three-stage process. At the first stage, the image is smoothed, at the second stage, it is segmented (a binary image is obtained), and, at the third stage, closed contours of pixel width are found in the binary image.
In this scheme, delta segmentation (DS) is the main process. Different methods are used as smoothing filters: ordinary low frequency filtering (LFF), median filtering, or Gauss filtering. The smoothing allows one to eliminate additive and pulse noises. At the second stage, the image is binarized using the DS. At the final stage, one-pixel-width closed contours are obtained using binary images.

2. DS METHOD

The DS algorithm is referred to threshold methods image segmentation and based on the dynamical determination and then variation of the threshold value, depending on the statistical characteristics of the brightness of the image in a certain window.
The statistical characteristics of the image brightness are

calculated in the window $W_{i,j}$ with the center (i, j) of dimension 3x3 pixels, which is moved through the image, from left to right and from top to bottom. For horizontal and vertical movements, steps of one pixel are used. The window W should not have the shape of a square and dimension 3 x 3, and the step of displacement may be greater than one pixel.

The main idea of the DS algorithm consists in dynamically finding the threshold value, which determines the cutting of the image.

To calculate it, we use an estimate based on the mean value $\widehat{\mathrm{Im}}_{i,j}$ of the pixels the window $W_{i,j}$ and the value of the mean square deviation $\sigma^2_{i,j}$ of the intensity in the window $W_{i,j}$ calculated by the known formulas of probability theory

$$\widehat{\mathrm{Im}}_{i,j} = \frac{1}{9}\sum_{p=i}^{i+2}\sum_{q=j}^{j+2}\mathrm{Im}_{p,q}$$

$$\sigma^2_{i,j} = \frac{1}{8}\sum_{p=i}^{i+2}\sum_{q=j}^{j+2}(\widehat{\mathrm{Im}}_{i,j} - \mathrm{Im}_{p,q})^2$$

where $\mathrm{Im}_{i,j}$ is the value of the intensity of an image pixel with the coordinates i and j, and $\mathrm{Im}_{p,q}$ are images with the coordinates relative to the center of the window $W_{i,j}$. Let us introduce several auxiliary quantities applied for determining the value of a dynamic threshold. The quantity $\varepsilon_{i,j}$ is calculated as

$$\varepsilon_{i,j} = \widehat{\mathrm{Im}}_{i,j} + \alpha\sigma^2_{i,j} \qquad (1)$$

where α is a certain constant that is determined empiricaly.

The subscript l numerates the steps of the algorithm in the course of motion of the window $W_{i,j}$ through the image $\mathrm{Im}_{i,j}$, as $l = i \times n + j$; $i = \overline{0,(n-1)}$, $j = \overline{0,(m-1)}$. Let us calculate the value of the error e_l; i.e., the difference between the value of the intensity of the central pixel in the window $W_{i,j}$ and the value of the dynamic threshold Y_{l-1} for the preceding pixel

$$e_l = \mathrm{Im}_{i,j} - Y_{l-1} \qquad (2)$$

At the initial stage of the DS, we have $Y_l = 127$, which corresponds to the middle of the interval of intensity values [0, 255]. At the end of each step of the algorithm, the current value of the threshold Y_{l-1} calculated by (4) is assigned to the value of the threshold at the preceding step Y_l. Note that the value of the error e_l, is calculated for each step of the algorithm, and the auxiliary quantity ε_{ij} is calculated once for each window. In the cases when the width of the window W is more than three points, the value of I he displacement step may be more than one pixel.

Then, we calculate the value of the auxiliary quart tity L_l, at the l-th step, which determines the value of the threshold

$$L_l = \begin{cases} 1, & e_l > \varepsilon_{i,j} \\ -1, & e_l < -\varepsilon_{i,j} \\ 0, & -\varepsilon_{i,j} \le e_l \le \varepsilon_{i,j} \end{cases} \qquad (3)$$

The value of the dynamic threshold Y_l at the l-th step is calculated as

$$Y_l = Y_{l-1} + \beta \times \varepsilon_{i,j} \times (L_l + L_{l-1}) \qquad (4)$$

where β is a constant that is determined empirically.

Next, we calculate the resulting value at the output of

$$g_l = \begin{cases} 0, & e_l > 0 \\ 1, & e_l < 0 \end{cases} \qquad (5)$$

The quantity L_l is zero at the beginning of each row. At the end of each step l, the value L_l is assigned to the value of the variable L_{l-1}. Figure 1 presents the general block diagram of the DS. The block labeled by the symbol ε_{ij} performs a calculation using formula (1), the block $\oplus$ calculates the error (2), the block with the step symbol executes (3), the block with the symbols Y_l and g_l performs calculations by formulas (4) and (5), and the block with the symbol τ performs a delay of one pixel. The result of the complete passage through the image is a binary image that has two intensity grades 0 and 1.

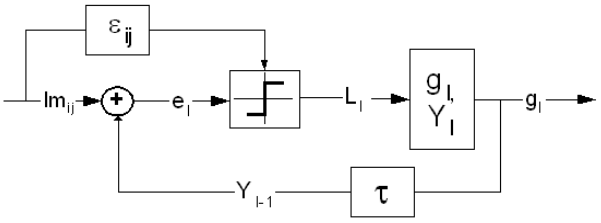

Fig. 1. The Block diagram of delta segmentation.

The algorithm for obtaining the contour is based on the method for computing the fundamental Minkowski subtraction operator [8] and is defined based on the morphological erosion operator. Morphological operations represent a nonlinear method for image processing. They are usually used to change the shape or to detect edges of objects. These operations are similar to convolution operations in the theory of linear filtering. In other

words, using the image $\mathrm{Im}_{i,j}$, the structuring element $B_{p,q}$ and a certain function, the resulting image $\widetilde{\mathrm{Im}}_{i,j}$ is computed. As a structuring element, we use four- or eight-connected regions shown in Figure 2.

Fig. 2. Example of four- or eight-connected regions for a structuring element B.

The process of finding contours is based on the calculation of the operator of removing interior points of graphical objects—the remove operator [7]. The function that implements the "morphological convolution" in the DS algorithm is constructed using the four-connected structuring element according to the following scheme. When the structuring element passes through the image from left to right and from top to bottom, zero is assigned to the pixels of the image $\mathrm{Im}_{i,j}$, for which four adjacent vertical and horizontal pixels are equal to one. As a result of application of this morphological filtering, only the pixels that belong to the boundary do not have zero value. The specific feature of this morphological operation is the one-pixel width of all closed contours.

3. SEQUENCE OF OPERATION

Thus the input image incoming from the video camera, passes preliminary processing. It consists at a removing noise, transformation of the image in black-and-white with DS, receiving of contours of objects, transformation of contours to sequence of points with coordinates ***(x,y)***, construction of contour function on the basis of the signature analysis as is showed in Figure 1 [8], loading fragment of contour function of the sample and further identification of the shape of object on the basis of geometrical correlation [9,10]. Example of moving radius-vector from center of gravity to points of contour for building contour function of real gear show in Figure 3.

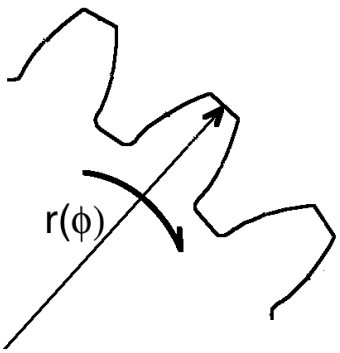

Fig. 3. Part of gear contour. Radius vector from centrum of gravity moving along this contour. In the result we receive contour function.

Then the sample is loaded into system in the form of a fragment of object (in this case it will be one of the tooth of gear). The contour function sequency compared with sample with assistance one of metrics based on geometric correlation [9].

These methods allow identifying the shape of object or a fragment of this shape with any beforehand set by accuracy. To control the accuracy of the parts, the modified method with automatic location of the contour fragments (ALCF) [9] is used, in which the fragments of the sample are compared with those of the tested part. Depending on the number of gear teeth and the required measurement accuracy, we will use a different number of symmetrically arranged fragments, as shown in Figure 5. In the simplest case, if the number of teeth is even, then it is enough to have two diametrically located gear contour parts for measurement, and control at the same time for two teeth. In the case of an odd number of teeth, only one of the two fragments will be used for control.

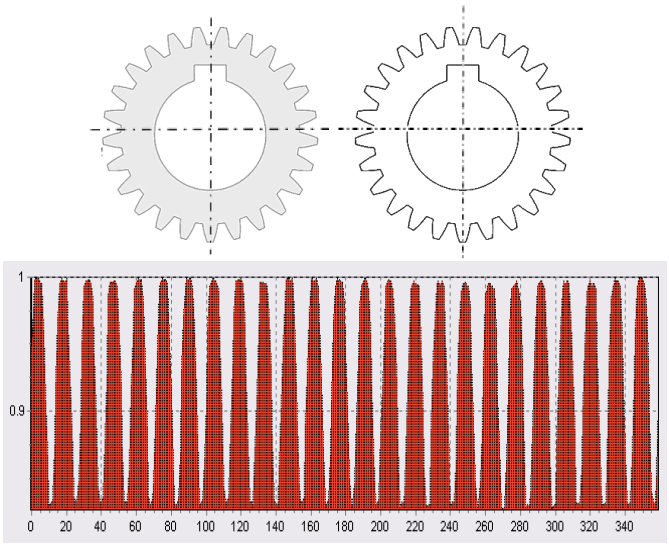

Fig. 4. Gear image, its contour, and the normalized contour function for the external contour (sweep).

Recall that the normalized contour function r is calculated by the points forming the perimeter of the object, and is defined in the polar coordinate system at a set of points in the range of angles $\left[0,360^{\circ}\right]$. It has a domain of variation $[0,1]$ and in the discrete case contains a fixed number of points M, a multiple of 360. The full definition of contour functions (r-functions) and methods for identifying objects based on them are described in [9], and an example of it for a gear is shown in Figure 4.

After calculating the contour function, it is no longer necessary to use systems of opposite intervals as in the ALCF methods, since in the simplest case, only one interval can be used to control accuracy. This reference interval will be sequentially compared with the contour function of the current object to

determine where the contour function fragment deviates from the reference fragment by an unacceptable value. For comparison, a fragment uses a specially developed metric, the formalisation of which is set forth below.

4. ACCURACY CONTROL METRIC

Definition 1. Suppose there is a contour function r defined on G. Since the shape will be controlled in a small segment of the contour, we define the set of points as G_p. Since more than one contour can be used to speed up the control, their description will be

$$g_l^p = \left[\tau_l^{'}, \tau_l^{''}\right], \quad l = \overline{1, L}; \quad G_p = \bigcup_{l=1}^{L} g_l^p,$$

$$g_l^p \bigcap g_m^p = \varnothing, l \neq m,$$

where L is the number of the used intervals. The width and position of g_l^p with respect to g_{l+1}^p for two and more intervals will be defined as

$$\tau_{l+1}^{'} = \tau_l^{'} + 360^{\circ} / L, \quad L \geq 1$$

$$\left|\tau_l^{''} - \tau_l^{'}\right| = \left|\tau_m^{''} - \tau_m^{'}\right| \quad \forall l, m = 1, L \text{ and}$$

$$\tau_{l+1}^{'} = \tau_l^{'} + 360^{\circ} / L, \quad L \geq 2;$$

The initial position g_l^p is fixed and determined by the displacement ψ

$$\tau_1^{'} = \psi; \quad \psi \in \left[0, 360^{\circ} / L\right], \quad L \geq 1$$

where L is the number of used intervals within the segment $\left[0, 360^{\circ}\right]$ and the argument τ always obeys the rule $\tau + 360^{\circ} = \tau$. Examples of such intervals on a circle for $L = 2, 3, 4, 5, 6$, are shown in Figure 5.

Definition 2. Let the contour function $x(\varphi)$ (sample) be defined in G_p, and the function $y(\varphi)$ (object) be defined in the interval $\left[0, 360^{\circ}\right]$ in a polar coordinate system. Let us introduce $\eta_{xy}(\varphi, \tau)$ as a partial function of difference of x and y values in the interval $\left[0, 360^{\circ}\right]$

$$\eta_{xy}(\varphi, \tau) = x(\varphi) - y(\tau - \varphi), \ \varphi \in G_p, \ \tau \in \left[0, 360^{\circ}\right]. \quad (6)$$

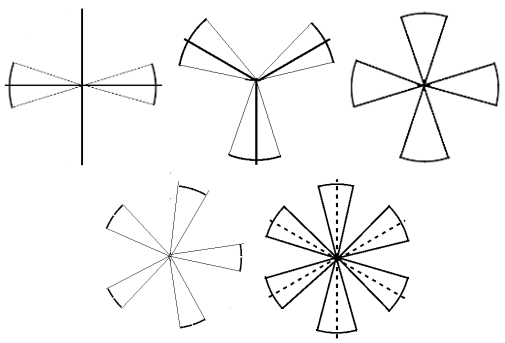

Fig. 5. Examples of opposite intervals in circumference for l = 2–6.

The formula (6) means that the difference of two values of two functions is calculated only on the set of contour intervals $g \subset G_p$, although $y(\varphi)$ is defined in $\left[0, 360^{\circ}\right]$.

Definition 3. The partial function of deviation $\delta_{xy}(\tau)$ of x from y is calculated at discrete points on G_p

$$\delta_{xy}(\tau) = \frac{1}{\left(\tau_l^{''} - \tau_l^{'}\right)} \sum_{\varphi \in G_p} \left|\eta_{xy}(\varphi, \tau)\right|,$$

$$\varphi \in G_p, \ \tau \in \left[0, 360^{\circ}\right]. \quad (7)$$

Definition 4. The partial function of mean deviation $\sigma_{xy}(\tau)$ of x from y is expressed as

$$\sigma_{xy}(\tau) = \frac{1}{\left(\tau_l^{''} - \tau_l^{'}\right)} \sum_{\varphi \in G_p} \left|\delta_{xy}(\tau) - \eta_{xy}(\varphi, \tau)\right|,$$

$$\varphi \in G_p, \ \tau \in \left[0, 360^{\circ}\right] \quad (8)$$

Definition 5. For the function $\delta_{xy}(\tau)$ calculated according to Eq. (7) on the set G_p *the function of precision contro*l 1 (FPC1) is expressed as

$$\lambda_{f1}(\tau) = \begin{cases} 1, & \left(\min\limits_{\tau} \delta_{xy}(\tau)\right) > \varepsilon_{f1}, \\ 0, & \left(\min\limits_{\tau} \delta_{xy}(\tau)\right) \leq \varepsilon_{f1}, \end{cases} \quad (9)$$

where ε_{f1} is the classification tolerance of FPC1, x .and y are the contour functions of the sample and identified object. In the absence of defects, FPC1 has the only value 0. Otherwise, the number of counts λ_{f1} corresponds to the number of imperfect gear teeth and the parameter τ corresponds to the angle of rotation with respect to the sample, where the defect is located.

Definition 6. For the function $\sigma_{xy}(\tau)$ calculated according to Eq. (8) on the set G_p the *function of precision control* 2 (FPC2) is expressed as

$$\lambda_{f2}(\tau) = \begin{cases} 1, & \left(\min\limits_{\tau} \sigma_{xy}(\tau)\right) > \varepsilon_{f2}, \\ 0, & \left(\min\limits_{\tau} \sigma_{xy}(\tau)\right) \leq \varepsilon_{f2}, \end{cases} \quad (10)$$

where ε_{f2} is the classification tolerance of FPC2, x and y are the contour functions of the sample and identified object. Here the values of λ_{f2} are analogous to the previous case, however, the function is more sensitive to the deviation of tooth shape from the necessary profile.

In the case of practical implementation (9) and (10) of the functions λ_{f1} and λ_{f2} for certain angle τ in the simplest case $L = 1$ in the interval $g_l^p = \left[\tau_l^{'}, \tau_l^{''}\right]$ the values of $\delta_{xy}(\tau)$ and $\sigma_{xy}(\tau)$ are calculated. Then a shift

occurs by the angle $\Delta\tau$, the value of which is determined by the precision of measurements carried out. Commonly the shift by 1° is used, but the values of 0.5°, 0.25° and smaller can be used for higher precision with the corresponding number of points of the contour function 720, 1440, etc. Obviously, when the sample segment will move along the contour function, the values of the metrics $\rho_1 = \min_{\tau} \sigma_{xy}(\tau)$ and $\rho_2 = \min_{\tau} \delta_{r_s, r_o}(\tau)$ will strongly oscillate. The minima of metric values will correspond to the positions, in which the fragment of the tooth contour function will coincide with the current position of the contour function of the gear tested. At some rotation angles, the coincidence will be complete and the metric value will be minimal. If this value exceeds the value of the classification tolerance ε_{f1} or ε_{f2}, then the shape of this tooth does not correspond to the specified tolerances. Thus, after a complete revolution of the sample fragment with respect to the object the functions $\lambda_{f1}(\tau)$ and $\lambda_{f2}(\tau)$ will record the angles, for which the specified geometry is not valid. Otherwise, the values of the functions λ_{f1} and λ_{f2} will be identically equal to 0.

5. DISCUSSION

Of course, the proposed shape control methodology is directly applicable only to certain types of gears, for example, to cylindrical spur gears, for both external and internal teeth. However, with some modification of this technology, which consists in positioning objects of control relative to the camera, it is possible to extend this technology to cylindrical oblique spur gears and bevel gears with straight and curved teeth and even to hypoid and spiroid gears with straight and oblique teeth [12-14]. Also, if the methodology is changed, so that the object will be placed on a support with a change in its position (for example, rotation) relative to the camera, it is possible to control the geometry of the worm shafts and gear racks with straight and oblique teeth.

The second direction in which this technology can be applied to control the shape of gear wheels is the deformation of the gear in the heat treatment process [15]. It is known that with such a deformation it is possible to change the dimensions of the gears, for example, around the circumference of the projections, the pitch of the teeth or the length of the common normal. The deformation of the shape of gear wheels around the circumference is shown in Figure 6.1, and the distortion of the "bevel" and "cone" type in Figure 6.2.

These types of deformations are easily detected using identification methods based on geometric correlation methods outlined in [11].

The biggest advantage here is the fact that there is no need to strictly position the camera relative to the object of control. The disadvantages of the proposed technology include the need to use special lighting to obtain clear images with the required resolution. In addition, this technology is not applicable to chevron gears.

It is necessary to notice, that accuracy of identification or accuracy of the control of the shape of object depends on the size of the fragment used as the sample. However, at the traced experiments it was visualize, that accuracy remains practically constant over a wide range of size of a fragment of the sample.

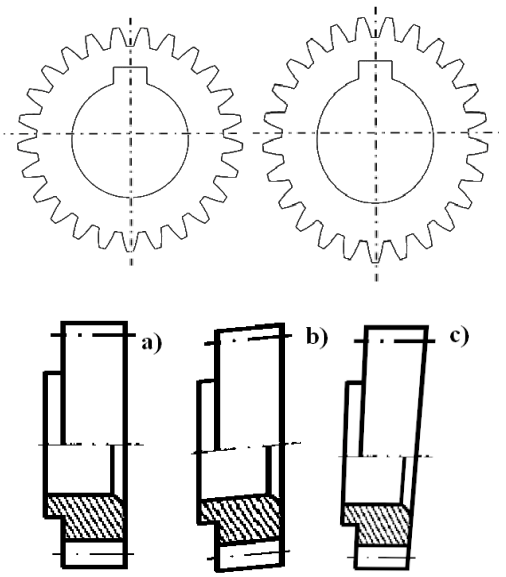

Fig 6. Deformation of gears during heat treatment. On the top, there is a deformation of the shape of a circle, on the bottom with a distortion like "bevel" and "cone". (Strongly exaggerated).

One of key questions in the offered methods is the value of error at the control of the shape of object. It is clear, that at numerous measurements the value of the metrics will vary in some bounds. This variability submits to the normal law of distribution [16,17] with experimentally defined values of an expectation and a variance as shown on Figure 7.

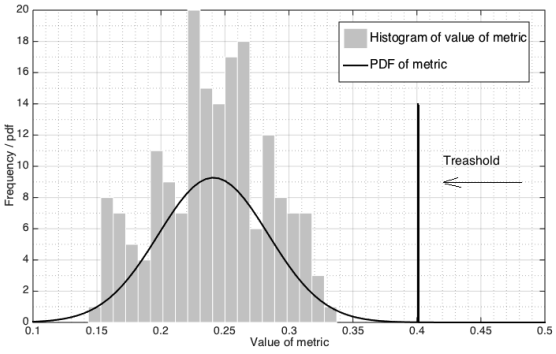

Fig 7. Histogram of metrics values, probability density function (pdf) and example of threshold allocation.

On the basis of the certain parameters of probability density function it is possible to assign value of the classification tolerance at the preset probability of an error of classification. Its value gets out experimentally and in the further for the predetermined parameters of the control of the shape does not change. However, it is necessary to notice, that the introduced methods possess high sensitivity, that is probability density function of metrics are very compact and therefore accuracy of the control in addition can be defined by value of the classification tolerance.

6. CONCLUSION

Using introduced video measuring system allows reducing essentially manufacturing flaw and industrial expenses due to:
-The fast control of all details over a party;
-Carrying out of measurements in shop-floor conditions in immediate proximity from machine tools;
-Online automatic check of a detail on conformity to shape admissions;
-Instant reception of the result on measurements;
-Detection of attributes of stitching of the tool for duly updating work of the processing machine tool;
-Service by one control system of the big park machine the equipment.
The proposed methodology for controlling the shape of geometrically correct centrally symmetric objects can be significantly extended to other objects that do not have axes of symmetry. In this case, in addition to the methods described, it is possible to use other metrics without using signature analysis, for example, based on DTW metrics [18]. Despite some shortcomings, this technology may in some cases be preferable compared to others.

7. REFERENCES

1. Gitin M. Maitra, (1994). *Handbook of Gear Design.* (Tata McGraw-Hill Education) 536.
2. Myszka, D. H., (2012). *Machines & Mechanisms: Applied Kinematic Analysis.* (University of Dayton 4th Edition), 385.
3. Davis, J.R., (2005). *Gear Materials, Properties and Manufacture.* (ASM International, Materials Park).
4. Oberg, E., Franklin, D., Horton, H.L.; Ryffel, H.H., (2000). *Machinery's Handbook*. (Publisher Industrial Press Inc., New York), 638.
5. Shigley, J.E., (2011). *Gearing: A Mechanical Designers' Workbook.* (McGraw-Hill), 1108.
6. Serra, J., (1982). *Image analysis and mathematical morphology.* (Academic Press, New York), 610.
7. Hendriks, L.C. L., Borgefors, G., Strand, R., (2013). *Mathematical Morphology and Its Applications to Signal and Image Processing. (*Proceedings ISMM Springer), 544.
8. Gonzales, R., Wintz, P., (1987). *Digital Image Processing.* (Addison Wesley), 503
9. Gostev, I. M., (2004). *Recognition of graphic patterns: Part I.* J. of Comp. and Syst. Sci. Int., V.43(1), 129-135.
10. Gostev, I., (2014). *About variability of using of methods of the shape identification based on geometrical correlation.* Advanced Materials Research, 837, 381-386.
11. Gostev, I.M., (2005). *Contour Fragment-Based Identification of Graphical Objects*. J. of Comp. and Syst. Sci. Int., 44(1), 135–142.
12. Lübben, T., Surm, H., Hoffmann, F., Zoch, H-W., (2016). *Identification of design related distortion of gear base bodies by experimental investigations*. Materialwissenschaft und Werkstofftechnik, 47(8), 678-687.
13. Kohlhoff, T., Prinz, C., Rentsch, R., Surm, H., (2012). *Influence of manufacturing parameters on gear distortion.* Materialwissenschaft und Werkstofftechnik, 43(1-2), 84-90.
14. Schülerm, A., Kleff, J., Heuer, V., Schmitt, G., and Leist, T., (2016), *Distortion of Gears and Sliding Sleeves for Truck Gear Boxes – A Systematical Analysis of Different Heat Treatment Concepts HTM.* Journal of Heat Treatment of Materials, 71(2), 90-98.
15. George, J.P., Koshy, J., Abraham, B.C., (1990), *Distortion Reduction in Gear Heat Treatment Process by a Simple Fixture.* International Journal of Emerging Technology and Advanced Engineering, 4(11), 306-312.
16. Fukunaga, K., (1990). *Introduction to Statistical Pattern Recognition*. Academic Press, New York, Nauka, Moscow, 592.
17. Gostev, I.M., (2004). *On Simulation and Estimation of Classification Tolerance*. Vestn. RUDN, Ser. Prikl. Comput. Matem., 3, 85–92.
18. Keogh, E., Chu, S., Hart, D., Pazzani, M., (2001). *An Online Algorithm for Segmenting Time Series*. IEEE Conference on Data Mining, 289-296.

Received: December 05, 2018 / Accepted: June 15, 2019 / Paper available online: June 20, 2019 © International Journal of Modern Manufacturing Technologies.